

Note on two-point mean square displacement

Naoya Katayama¹ and Takahiro Sakaue¹

¹*Department of Physical Sciences, Aoyama Gakuin University, 5-10-1 Fuchinobe, Chuo-ku, Sagami-hara, Japan**

When probe molecules of interest are embedded in a container or aggregate under stochastic motion, one needs to rely on the so-called two-point mean square displacement (MSD) measurement to extract the intrinsic mobility of the probes. We discuss two versions, based on the time series of *relative vector* or *distance* between two probes, and summarize their basic properties compared to the standard MSD. We also propose a way to extract (i) the non-Gaussianity in the displacement statistics and (ii) the motional correlation between probes from the two-point MSD. The results are presented not only for independent probes, but also for intramolecular probes within a long polymer, which could be useful in quantifying the dynamics of chromatin loci in living cell nucleus.

Single particle tracking is a method of analysis widely used in material and biological sciences [1, 2]. By attaching a fluorescent tag to the molecule of interest, it enables us to observe and record its real time motion under an optical microscope [3, 4]. The motional characteristics thus obtained are expected to carry a rich information on the system. In typical applications, one calculates from the stochastic trajectory $\vec{r}(t)$ the mean-square displacement (MSD);

$$\text{MSD}(\tau) \equiv \langle |\Delta\vec{r}(\tau)|^2 \rangle \quad (1)$$

where $\Delta\vec{r}(\tau) = \vec{r}(t_0 + \tau) - \vec{r}(t_0)$. MSD thus measures the typical displacement squared during the time interval τ . Note that MSD generally depends on the time origin t_0 . In the present note, we assume stationary state, where time translational invariance implies no dependence of statistical quantities on t_0 , and $\langle \dots \rangle$ represents the average over trajectories and over the time origin t_0 .

Although calculation of MSD using Eq. (1) looks quite straightforward, one may encounter situations, often in the measurement in biological samples, where it is not the case. Indeed, a complication arises when the molecule of interest is embedded in a medium (container or aggregate), which itself moves. The best example is found in the analysis of chromatin dynamics inside a cell nucleus [8–17]; we are interested in the motion of chromatin locus, but the time series of its position reflects not only the intrinsic chromatin dynamics, but also the translational and rotational motion of the nucleus, which is subjected to the random or systematic forces from cytoplasm, see Fig. 1. While such an effect of the nuclear motion might be negligible in short time scale, it becomes increasingly visible in longer time scale. For instance, in early embryos of *C. elegans*, the nuclear motion dominates the apparent motion of chromatin locus already at $\tau \sim 10$ seconds [11]. A natural strategy here to extract the intrinsic chromatin mobility is to make use of the trajectories of two probes. The same problem is encountered in many other cases, for instance, when analyzing the motion of individual cells within multicellular aggre-

gates. With such a situation in mind, Pönisch and Zaburdaev have recently studied the statistics of the relative distance between independently moving Brownian particles [5]. In the chromatin problem, the polymeric effect should be taken into account, in which one may look at not only independently moving intermolecular pair but also intramolecular pair, see Fig. 2 [13, 14, 16, 17].

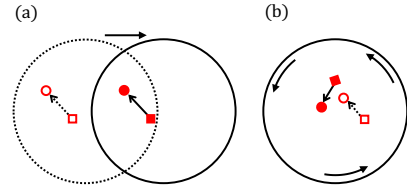


FIG. 1. Schematics illustrating the effect of (a) translational or (b) rotational motion of a container on the relative vector $\vec{d}(t)$ and the distance $d(t)$. Intrinsic mobility of probes are hypothetically set to zero to emphasize the extrinsic effect.

Let $\vec{r}_1(t)$ and $\vec{r}_2(t)$ to represent the positions of the two probes at time t . The method of analysis using $\vec{r}_1(t)$ and $\vec{r}_2(t)$ to quantify the intrinsic mobility of probe may be called *two-point MSD* analysis. In literature, there are two variants of the two-point MSD analysis, which differ in the definition of the analyzed quantities, i.e., one may look at the time series of either a relative vector $\vec{d}(t) = \vec{r}_1(t) - \vec{r}_2(t)$ connecting two probes or its absolute value $d(t) = |\vec{d}(t)|$, the latter being a distance between the probes. In this note, we aim to clarify the similarity and difference between these two analyses, and their quantitative connection to the standard MSD. In Sec. I, we first define the quantities considered in two-point MSD analysis. We then briefly review the case with two independently moving probes in Sec. II. We proceed in Sec. III to the intramolecular analysis, in which two probes belong to the common polymer chain, i.e., two loci in the same chromatin. Sec. IV is devoted to discussion on the general aspect of two-point MSD. We also demonstrate that the method can be applied to quantify the non-Gaussian parameter in the displacement statistics and the motional correlation of probe pair.

* corresponding author, sakaue@phys.aoyama.ac.jp

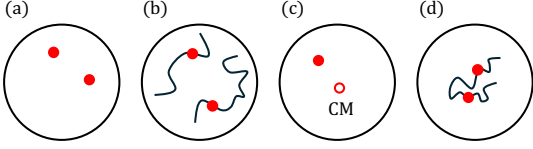


FIG. 2. Possible variations for a pair of probes in two-point MSD measurement. (a) and (b): Pair of independent probes; while probes are simple particles in (a), tagged monomers play a role of probe in (b), each of which belongs to different polymers. (c) Instead of the second probe, one can make use of the center of mass position $\vec{r}_c(t)$ (or other fixed point) in the moving container to define a vector $\vec{d}(t) = \vec{r}_1(t) - \vec{r}_c(t)$. (d) Intramolecular probe pair as an example of mutually dependent probes.

I. QUANTITIES ANALYZED IN TWO-POINT MSD

We define the mean-square change in the relative vector \vec{d} (MSCV) as

$$\text{MSCV}(\tau) \equiv \langle |\Delta \vec{d}(\tau)|^2 \rangle \quad (2)$$

with $\Delta \vec{d}(\tau) = \vec{d}(t_0 + \tau) - \vec{d}(t_0)$. Similarly, we define the mean-square change in the distance $d = |\vec{d}|$ (MSCD) as

$$\text{MSCD}(\tau) \equiv \langle [\Delta d(\tau)]^2 \rangle \quad (3)$$

with $\Delta d(\tau) = d(t_0 + \tau) - d(t_0)$. An important difference between these quantities is found by observing that MSCV excludes only the translational, but not the rotational motion of the container, see Fig. 1. Thus, the MSCD is more suitable when the rotational motion of the container is non-negligible.

II. INDEPENDENTLY MOVING PROBES

A. Relative vector analysis

Consider probes performing Brownian motion in three dimensional space. The probability density function of position \vec{r}_i of each probe ($i = 1, 2$) with diffusion coefficient D_i and initial position \vec{r}_{i0} is

$$P_i(\vec{r}_i, \tau | \vec{r}_{i0}) = \frac{1}{(4\pi D_i \tau)^{3/2}} \exp\left(-\frac{|\vec{r}_i - \vec{r}_{i0}|^2}{4D_i \tau}\right) \quad (4)$$

Then, MSD of each probe is

$$\text{MSD}_i(\tau) = \int d\vec{r}_i |\Delta \vec{r}_i(\tau)|^2 P_i(\vec{r}_i, \tau | \vec{r}_{i0}) = 6D_i \tau \quad (5)$$

Without loss of generality, we set $\vec{r}_{10} = (0, 0, d_0)$, $\vec{r}_{20} = (0, 0, 0)$. From Eq. (4), the probability density function $P_{\vec{d}}(\vec{d}, \tau)$ of relative vector $\vec{d} = \vec{r}_1 - \vec{r}_2 = (d_x, d_y, d_z)$ is

obtained as

$$\begin{aligned} P_{\vec{d}}(\vec{d}, \tau | \vec{d}_0) &= \int d\vec{r}_2 P_1(\vec{r}_2 + \vec{d}, \tau | \vec{r}_{10}) P_2(\vec{r}_2, \tau | \vec{r}_{20}) \\ &= \frac{1}{(4\pi D^* \tau)^{3/2}} \exp\left(-\frac{d_x^2 + d_y^2 + (d_z - d_0)^2}{4D^* \tau}\right) \end{aligned} \quad (6)$$

This is a well-known result, i.e., in the rest frame of probe 2, the motion of probe 1 looks as Brownian motion with diffusion coefficient $D^* = D_1 + D_2$ [6, 7], where, for generality of argument, we introduce the relative diffusivity D^* . It then follows

$$\text{MSCV}(\tau) = \int d\vec{d} |\Delta \vec{d}|^2 P_{\vec{d}}(\vec{d}, \tau | \vec{d}_0) = 6D^* \tau. \quad (7)$$

which results in twice the MSD if $D_1 = D_2$, i.e., $\text{MSCV}(\tau) = 2\text{MSD}(\tau)$ for two independent identical probes, see Fig. 3 (c).

B. Distance analysis

Pönisch and Zaburdaev have presented a detailed analysis on the statistics of distance d between two independent Brownian particles in two dimension [5]. Following their analysis, here we present the result in three dimension. First, we transform the probability density function (6) of relative vector \vec{d} to that of distance d ;

$$\begin{aligned} P_d(d, \tau | d_0) &= \int d\vec{d} P_{\vec{d}}(\vec{d}, \tau | \vec{d}_0) \delta\left(d - \sqrt{d_x^2 + d_y^2 + d_z^2}\right) \\ &= \frac{d}{d_0 \sqrt{4\pi D^* \tau}} \left[\exp\left(-\frac{(d - d_0)^2}{4D^* \tau}\right) - \exp\left(-\frac{(d + d_0)^2}{4D^* \tau}\right) \right] \end{aligned} \quad (8)$$

The time evolution of $P_d(d, \tau | d_0)$ is shown in Fig. 3 (a), where the width of the distribution grows as $\sim \tau^{1/2}$. From Eq. (8), we calculate the MSCD under the condition $d(0) = d_0$;

$$\begin{aligned} \text{MSCD}(\tau | d_0) &\equiv \int_0^\infty dd (d - d_0)^2 P_d(d, \tau | d_0) \\ &= 6D^* \tau + 2d_0^2 - 4d_0 \sqrt{\frac{D^* \tau}{\pi}} \exp\left(-\frac{d_0^2}{4D^* \tau}\right) \\ &\quad - 2(2D^* \tau + d_0^2) \text{erf}\left(\frac{d_0}{\sqrt{4D^* \tau}}\right) \end{aligned} \quad (9)$$

Unlike MSD and MSCV, this quantity depends explicitly on the initial condition, and this introduces the d_0 dependent time scale $\tau_d = d_0^2/4D^*$. With the asymptotic behavior of the error function, we find

$$\text{MSCD}(\tau | d_0) \simeq \begin{cases} 2D^* \tau & (\tau \ll \tau_d) \\ 6D^* \tau & (\tau \gg \tau_d) \end{cases} \quad (10)$$

Figure. 3 (b) summarizes the above result, where we plot how $\text{MSCD}(\tau; d_0) = \langle (d(\tau) - d_0)^2 \rangle_{d_0}$ evolves with time

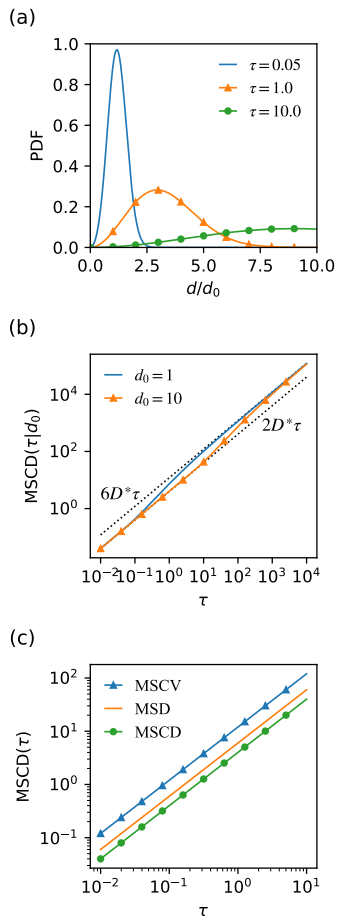


FIG. 3. Two-point MSD analysis for a pair of independent probes. (a) Time evolution of the probability density function $P_d(d, t|d_0)$ of the inter-probe distance d starting from $d(0) = d_0$. (b) Conditional $\text{MSCD}(\tau|d_0)$ as a function of lag time τ for two different initial separation d_0 . (c) $\text{MSCV}(\tau)$ and $\text{MSCD}(\tau)$ as a function of lag time τ compared to $\text{MSD}(\tau)$. In (b) and (c), the length is measured in unit of a (probe diameter) and the time is measured in unit of $a^2/2D^*$.

scale. We note that Eq. (10) is consistent with the result of Yesbolatova et al. [11] and that of Pönisch and Zaburdaev [5]. In the latter work, $6D^*\tau$ in long time-scale is replaced with $4D^*\tau$ in two dimensional systems.

From experimental standpoint, it would not be easy to take statistics with fixed d_0 . In typical experiments, one usually takes time averaging, where the time origin, and corresponding d_0 continuously change. With the distribution $p(d_0)$ of the initial separation d_0 during measurement, one thus defines

$$\text{MSCD}(\tau) \equiv \int_0^\infty dd_0 \text{MSCD}(\tau|d_0)p(d_0) \quad (11)$$

Using Eq. (10), we can evaluate $\text{MSCD}(\tau)$ as

$$\text{MSCD}(\tau) \simeq q_> \times 2D^*\tau + q_< \times 6D^*\tau \quad (12)$$

with

$$q_> = \int_{\sqrt{4D^*\tau}}^\infty p(d_0) dd_0, \quad q_< = \int_0^{\sqrt{4D^*\tau}} p(d_0) dd_0 \quad (13)$$

For a pair of free probes, the relative vector \vec{d} is uniformly sampled. If we tentatively introduce the maximum d_m for the allowed d_0 , then

$$p(d_0) = \frac{4\pi d_0^2}{4\pi d_m^3/3} = \frac{3d_0^2}{d_m^3} \quad (14)$$

For any given finite τ , $q_> \rightarrow 1$ and $q_< \rightarrow 0$ in large enough space $d_m \rightarrow \infty$. We thus find

$$\text{MSCD}(\tau) = 2D^*\tau \quad (15)$$

for two independently moving probes, see Fig. 2 (a). If two probes are identical, we find $\text{MSCD}(\tau) = 4D\tau = 2/3\text{MSD}(\tau)$.

C. Motion analysis in center-of-mass frame

Instead of tracking two probes, one can track the position of a single probe $\vec{r}_1(t)$ with respect to a particular fixed point in the moving container. A convenient choice for the fixed point would be the center of mass, whose position $\vec{r}_c(t)$ dynamically changes with the container's translation [15]. Similar to the two-probes tracking case, one can define the vector $\vec{d}(t) = \vec{r}_1(t) - \vec{r}_c(t)$, and its magnitude $d(t) = |\vec{d}(t)|$, see Fig. 2 (c). In order to avoid a possible confusion, let us attach a subscript “c” as MSCV_c and MSCD_c to indicate the quantities of interest in the center-of-mass frame analysis. Since the diffusivity of the fixed point (second probe) is obviously zero, the relative diffusion coefficient in this case is simply $D^* = D_1$. Thus, we find from Eq. (7)

$$\text{MSCV}_c(\tau) = 6D_1\tau = \text{MSD}(\tau) = \frac{1}{2}\text{MSCV}(\tau) \quad (16)$$

and from Eq. (15)

$$\text{MSCD}_c(\tau) = 2D_1\tau = \frac{1}{3}\text{MSD}(\tau) = \frac{1}{2}\text{MSCD}(\tau) \quad (17)$$

III. INTRAMOLECULAR PROBES

As an example of correlated pair of probes, we consider two tagged monomers belonging to a common polymer, see Fig. 2 (d).

Model— Our calculation in this section is based on the Rouse model. The polymer consists of N monomers connected through spring in series. The position of n -th monome $\vec{r}(n, t) = (x(n, t), y(n, t), z(n, t))$ evolves according to the Rouse equation of motion, which takes in continuum limit the following form

$$\gamma \frac{\partial \vec{r}(n, t)}{\partial t} = k \frac{\partial^2 \vec{r}(n, t)}{\partial n^2} + \vec{\xi}(n, t) \quad (18)$$

where the friction coefficient γ and the spring constant k defines the monomeric time scale $\tau_0 = \gamma/k$. The last term $\vec{\xi}(n, t)$ is uncorrelated Gaussian white noise acting on n -th monomer with $\langle \vec{\xi}(n, t) \rangle = \vec{0}$ and $\langle \vec{\xi}(n, t) \vec{\xi}(m, s) \rangle = 2\gamma k_B T \mathcal{I} \delta(n - m) \delta(t - s)$, which represents the effect of thermal noise, with $k_B T$ being the thermal energy and 3×3 identity matrix \mathcal{I} .

In what follows, we neglect the chain end effect assuming large N . Then, starting from an initial configuration $\vec{r}(n, t_0)$ at time t_0 , the solution is obtained as

$$\begin{aligned} \vec{r}(n, t) = & \frac{1}{\gamma} \int dn' \int_{t_0}^t dt' G(n - n', t - t') \vec{\xi}(n', t') \\ & + \int dn' G(n - n', t - t_0) \vec{r}(n', t_0) \end{aligned} \quad (19)$$

with the Green function

$$G(n, t) = \sqrt{\frac{\gamma}{4\pi kt}} \exp\left(-\frac{\gamma}{4kt} n^2\right) \quad (20)$$

Mean square displacement— Let us define the time correlation function of fluctuation $\delta x(n, t) = x(n, t) - \langle x(n, t) \rangle$ of a tagged monomer;

$$C_0(t_0, t_1, t_2) \equiv \langle \delta x(n, t_1) \delta x(n, t_2) \rangle \quad (21)$$

Note that this quantity generally depends on the initial time t_0 in addition to the two observation times t_1 and $t_2 (\geq t_1)$. Using the solution (19), it is calculated as

$$\begin{aligned} C_0(t_0, t_1, t_2) &= \frac{2k_B T}{\gamma} \int_{t_0}^{t_1} dt' G(0, t_1 + t_2 - 2t') \\ &= \frac{k_B T}{k} \sqrt{\frac{1}{\pi \tau_0}} \left[(t_1 + t_2 - 2t_0)^{1/2} - (t_2 - t_1)^{1/2} \right] \end{aligned} \quad (22)$$

where we have used Eq. (20). From this, we obtain

$$\begin{aligned} & \langle (\delta x(n, t + \tau) - \delta x(n, t))^2 \rangle \\ &= C_0(t_0, t + \tau, t + \tau) + C_0(t_0, t, t) - 2C_0(t_0, t, t + \tau) \\ &\rightarrow \frac{2k_B T}{k} \sqrt{\frac{\tau}{\pi \tau_0}} \quad (t_0 \rightarrow -\infty), \end{aligned} \quad (23)$$

where in the final step, we focus on the stationary state by letting $t_0 \rightarrow -\infty$, which implies $x(n, t + \tau) - x(n, t) = \delta x(n, t + \tau) - \delta x(n, t)$. This leads to the well-known sub-diffusion scaling of MSD of each probe (with exponent 0.5 for a Rouse model) [18–20];

$$\begin{aligned} \text{MSD}(\tau) &= 3 \times \langle (x(n, t + \tau) - x(n, t))^2 \rangle \\ &= \frac{2a^2}{\sqrt{\pi}} \sqrt{\frac{\tau}{\tau_0}}, \end{aligned} \quad (24)$$

where we introduce the mean square bond length a^2 through equipartition theorem $k = 3k_B T/a^2$ and a factor 3 reflects the dimensionality (the number of components) and the isotropy of the space.

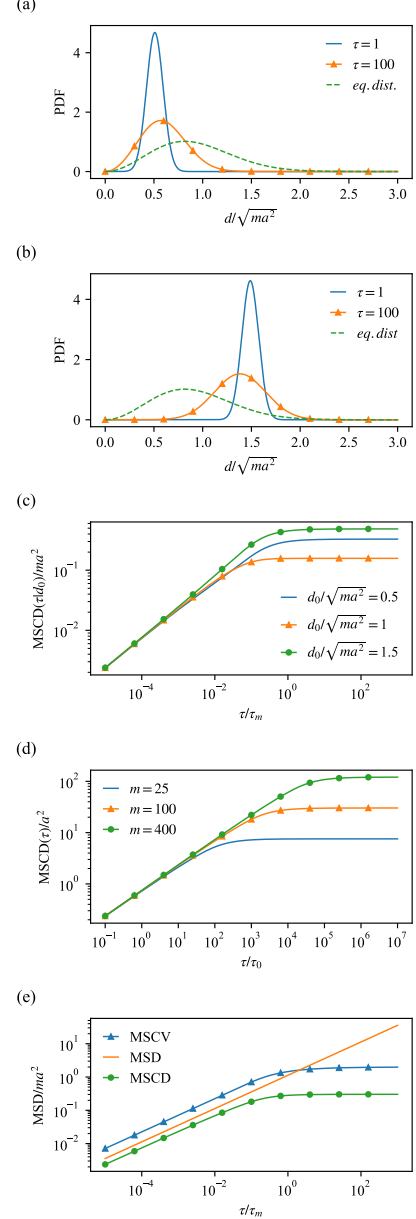


FIG. 4. Two-point MSD analysis for a pair of intramolecular probes. (a) and (b) Time evolution of the probability density function $P_d(d, t|d_0)$ of the inter-probe distance d starting from (a) $d(0) = d_0 = 0.5\sqrt{ma^2}$ and (b) $d(0) = d_0 = 1.5\sqrt{ma^2}$. Dashed curves represent the equilibrium distribution. (c) Conditional $\text{MSCD}(\tau|d_0)$ as a function of scaled lag time τ/τ_m for three different initial separation d_0 . (d) $\text{MSCD}(\tau)$ as a function of lag time τ for three different inter-probe separation m . (e) $\text{MSCV}(\tau)$ and $\text{MSCD}(\tau)$ as a function of scaled lag time τ/τ_m compared to $\text{MSD}(\tau)$.

Correlation and relaxation functions of relative vector— We label n_1 -th and n_2 -th monomers as two probes with their separation $m = |n_2 - n_1|$, and assume the stationary state. Central quantities in the following calculation are the time correlation function of

$$d_x(t) = x(n_1, t) - x(n_2, t);$$

$$C_{\vec{d}}(\tau) \equiv \langle d_x(t_1 + \tau) d_x(t_1) \rangle. \quad (25)$$

and the relaxation function

$$\tilde{h}(\tau) \equiv \frac{\langle d_x(t_1 + \tau) \rangle_{d_0}}{d_{x0}} \quad (26)$$

where $\langle \dots \rangle_{d_0}$ refers to the average over the sub-ensemble specified by the condition $d_x(t_1) = d_{x0}$. In stationary state, both depend only on the separation of probes m (aside from the neglected chain-end effect) and the time difference τ . In addition, these two quantities are related to each other via fluctuation-dissipation theorem [18];

$$\frac{ma^2}{3} \tilde{h}(\tau) = C_{\vec{d}}(\tau) \quad (27)$$

In Appendix A, we calculate the relaxation function

$$\tilde{h}(\tau) = \operatorname{erf} \left(\sqrt{\frac{\tau_m}{4\tau}} \right) - \sqrt{\frac{4\tau}{\pi\tau_m}} \left[1 - \exp \left(-\frac{\tau_m}{4\tau} \right) \right], \quad (28)$$

where we introduce $\tau_m \equiv \tau_0 m^2$, which corresponds to the relaxation time of a subchain of size m .

A. Relative vector analysis

Summing up contributions from each component, MSCV(τ) is calculated as

$$\begin{aligned} \text{MSCV}(\tau) &= 3 \times [(d_x(t + \tau) - d_x(t))^2] \\ &= 3 \times 2 [C_{\vec{d}}(0) - C_{\vec{d}}(\tau)] \\ &= 2ma^2 (1 - \tilde{h}(\tau)) \end{aligned} \quad (29)$$

Equation (29) is consistent with the result reported in Ref. [13].

Using limiting behavior of $\tilde{h}(\tau)$, we find

$$\text{MSCV}(\tau) \simeq \begin{cases} \frac{4a^2}{\sqrt{\pi}} \sqrt{\frac{\tau}{\tau_0}} & (\tau \ll \tau_m) \\ 2ma^2 & (\tau \gg \tau_m) \end{cases} \quad (30)$$

Comparing Eqs. (24) and (30), one find $\text{MSCV}(\tau) = 2\text{MSD}(\tau)$ in short time-scale regime ($\tau \ll \tau_m$), the same relation to the case of independent probes (Sec. II A), see Fig. 4 (e).

B. Distance analysis

We will follow the steps illustrated in Sec. IIB for the case of independent probes. We first need to find $P_{\vec{d}}(\vec{d}, \tau | \vec{d}_0)$; the probability density function of the relative vector \vec{d} at $t = t_1 + \tau$ given the condition $|\vec{d}(t = t_1)| = d_0$ in stationary state. Let $t_0 \rightarrow -\infty$ in Eq. (19), the system is thus in equilibrium at $t = t_1$. From this

equilibrium ensemble, we pick up a sub-ensemble filtered by the condition $\vec{d}(t_1) = d_0/\sqrt{3}(1, 1, 1)$. From here on, we measure the time as a function of $\tau = t - t_1$ since we are interested in the subsequent time evolution after the initial condition at $t = t_1$. The probability density function takes the form

$$P_{\vec{d}}(\vec{d}, \tau | \vec{d}_0) = \frac{1}{[2\pi g(\tau)]^{3/2}} \exp \left(-\frac{\sum_{\alpha=x,y,z} [d_\alpha - \langle d_\alpha(\tau) \rangle_{d_0}]^2}{2g(\tau)} \right) \quad (31)$$

where $\langle \dots \rangle_{d_0}$ refers to averaging over the sub-ensemble, and $g(\tau) \equiv \langle \{d_\alpha(\tau) - \langle d_\alpha(\tau) \rangle_{d_0}\}^2 \rangle$. Note that the ‘‘initial’’ separation at $\tau = 0$ shows only up through the first moment, i.e., the average time evolution $\langle d_\alpha(\tau) \rangle_{d_0}$ of each component ($\alpha = x, y, z$). In our ‘‘initial’’ condition, all the components follows the same average evolution, which is described using the relaxation function, see Eq. (26);

$$\langle d_\alpha(\tau) \rangle_{d_0} = \frac{d_0}{\sqrt{3}} \tilde{h}(\tau) \quad (\tau \geq 0, \alpha = x, y, z) \quad (32)$$

The variance $g(\tau) \equiv \langle \{d_\alpha(\tau) - \langle d_\alpha(\tau) \rangle_{d_0}\}^2 \rangle$ is calculated as

$$\begin{aligned} g(\tau) &= \langle [\{d_\alpha(\tau) - d_\alpha(0)\} + \{d_\alpha(0) - \langle d_\alpha(\tau) \rangle_{d_0}\}]^2 \rangle \\ &= \langle \{d_\alpha(\tau) - d_\alpha(0)\}^2 \rangle - \langle \{d_\alpha(0) - \langle d_\alpha(\tau) \rangle_{d_0}\}^2 \rangle \\ &= 2(C_{\vec{d}}(0) - C_{\vec{d}}(\tau)) - \frac{ma^2}{3} (1 - \tilde{h}(\tau))^2 \\ &= \frac{ma^2}{3} (1 - \tilde{h}(\tau)^2). \end{aligned} \quad (33)$$

where we have used Eq. (27) in the final step. Note that, to obtain the second term in third line, we have carried out the following averaging

$$\int_0^\infty dd_0 d_0^2 p(d_0) = ma^2 \quad (34)$$

with the equilibrium distribution of d_0 ;

$$p(d_0) = 4\pi \left(\frac{3}{2\pi ma^2} \right)^{3/2} d_0^2 \exp \left(-\frac{3d_0^2}{2ma^2} \right) \quad (35)$$

After variable transformation from \vec{d} to $d = \sqrt{|\vec{d}|^2}$, we obtain the probability density function of d conditioned on $d(0) = d_0$;

$$\begin{aligned} P_d(d, \tau | d_0) &= \frac{d}{d_0 \tilde{h}(\tau) \sqrt{2\pi g(\tau)}} \\ &\times \left[\exp \left(-\frac{(d - d_0 \tilde{h}(\tau))^2}{2g(\tau)} \right) - \exp \left(-\frac{(d + d_0 \tilde{h}(\tau))^2}{2g(\tau)} \right) \right] \end{aligned} \quad (36)$$

Figure 4 (a) or (b) show the time evolution of $P_d(d, \tau | d_0)$ starting from a shrunk ($d_0/\sqrt{ma^2} < 1$) or swollen

($d_0/\sqrt{ma^2} > 1$) conformation, respectively. Unlike for the case of independent probes, the distributions in both cases approach towards the equilibrium distribution given by Eq. (35) after $\tau \simeq \tau_m$. From this, we obtain the MSCD conditioned on $d(0) = d_0$, see Fig. 4 (c);

$$\begin{aligned} \text{MSCD}(\tau|d_0) &\equiv \int_0^\infty dd (d - d_0)^2 P_d(d, \tau|d_0) \\ &= 3g(\tau) + d_0^2(1 + \tilde{h}(\tau)^2) - d_0 \sqrt{\frac{8g(\tau)}{\pi}} \exp\left(-\frac{(d_0\tilde{h}(\tau))^2}{2g(\tau)}\right) \\ &\quad - 2 \left[\frac{g(\tau) + (d_0\tilde{h}(\tau))^2}{\tilde{h}(\tau)} \right] \text{erf}\left(\frac{d_0\tilde{h}(\tau)}{\sqrt{2g(\tau)}}\right) \end{aligned} \quad (37)$$

Comparing Eqs. (36) and (37), respectively, with Eqs. (8) and (9), it is clear how the connectivity effect comes in the statistical time evolution of inter-probe distance.

Experimentally, as discussed in Sec. II B, more easily accessible quantity is the time averaged MSCD, see Eq. (11), obtained by averaging over the equilibrium distribution of d_0 given by Eq. (35). After performing the averaging operation, we find

$$\begin{aligned} \frac{\text{MSCD}(\tau)}{ma^2} \\ = 2 - \frac{4}{\pi} \sqrt{1 - \tilde{h}(\tau)^2} \left[1 + \left(\omega(\tilde{h}) + \frac{1}{3\omega(\tilde{h})} \right) \arctan(\omega(\tilde{h})) \right] \end{aligned} \quad (38)$$

where we have defined $\omega(x) = \sqrt{x^2/(1-x^2)}$. Using limiting behaviors of $\tilde{h}(\tau)$, we find

$$\text{MSCD}(\tau) \simeq \begin{cases} \frac{4a^2}{3\sqrt{\pi}} \sqrt{\frac{\tau}{\tau_0}} & (\tau \ll \tau_m) \\ ma^2 \left(2 - \frac{16}{3\pi}\right) & (\tau \gg \tau_m) \end{cases} \quad (39)$$

Comparing Eq. (39) with Eq. (24), we find $\text{MSCD}(\tau) = 2/3\text{MSD}(\tau)$ in short time-scale regime ($\tau \ll \tau_m$), the same relation to the case of independent probes (Sec. II B), see Fig. 4 (e).

IV. DISCUSSIONS

A. General property of MSCV and MSCD

In Sec. II, we have seen the relation

$$\text{MSD}(\tau) = \frac{1}{2}\text{MSCV}(\tau) = \frac{3}{2}\text{MSCD}(\tau) \quad (40)$$

for two independently moving probes, see also Eqs. (16) and (17) for the analysis in the center-of-mass frame (Sec. II C). The analysis of Rouse model in Sec. III B shows that the same relation also holds for the intramolecular pair of probes in short-time scale ($\tau \ll \tau_m$). Although our analyses in these preceding sections are based on simple models, i.e., Brownian motion model in

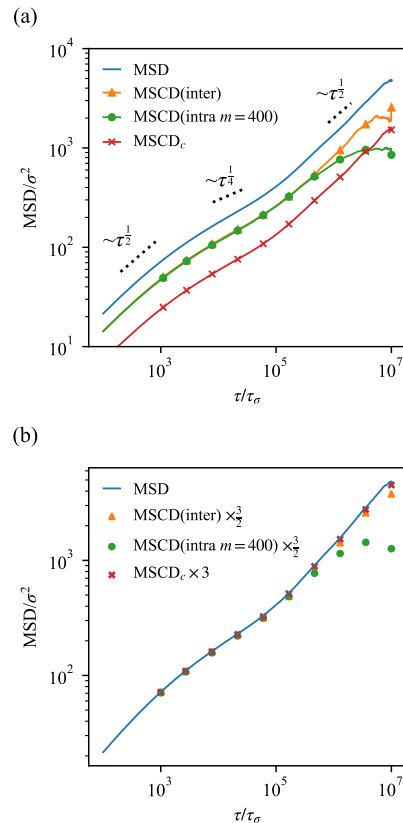


FIG. 5. Distance analysis performed for tagged monomer probes in entangled polymer solutions. (a) Shown are the following quantities as a function of lag time τ ; MSD of a tagged monomer, $\text{MSCD}(\text{inter})$ from two independent probes on different polymers, $\text{MSCD}(\text{intra})$ from two intramolecular probes, MSCD_c from a single probe and the center of mass. Selection of tagged monomer(s) along each chain (with length $N = 600$) is $n = 100$, or $(n_1, n_2) = (100, 500)$ for the intramolecular pair. (b) All the quantities shown in (a) collapse according to formulas (40) and (17).

Sec. II B and Rouse model in Sec. III B, we now discuss that the relation (40) is quite generally expected even for more complex situations, i.e., probe particles performing anomalous diffusion (see, for instance, Fig. 2 (b)) and probes belonging to more general polymers, etc., as a consequence of defining properties of MSCV and MSCD.

First, the relation between MSD and MSCV can be derived from the following simple argument. Since $\Delta \vec{d}(\tau) = \Delta \vec{r}_1(\tau) - \Delta \vec{r}_2(\tau)$, one can transform Eq. (3) as

$$\text{MSCV}(\tau) = \langle |\Delta \vec{r}_1(\tau)|^2 \rangle + \langle |\Delta \vec{r}_2(\tau)|^2 \rangle - 2\langle \Delta \vec{r}_1(\tau) \cdot \Delta \vec{r}_2(\tau) \rangle \quad (41)$$

Then, assuming that two probes are independent; $\langle \Delta \vec{r}_1(\tau) \cdot \Delta \vec{r}_2(\tau) \rangle = \langle \Delta \vec{r}_1(\tau) \rangle \cdot \langle \Delta \vec{r}_2(\tau) \rangle = 0$, and have the same diffusivity, one finds $\text{MSCV}(\tau) = 2\text{MSD}(\tau)$.

For the relation between MSD and MSCD, we start from a relation $\vec{d}(t_0 + \tau) = \vec{d}(t_0) + \Delta \vec{r}_1(\tau) - \Delta \vec{r}_2(\tau)$, and introduce a unit vector \hat{u} associated with the relative

vector at $t = t_0$, i.e., $\vec{d}(t_0) = d_0 \hat{u}$, see also Refs. [5, 11] for a related discussion. Then, the distance at time $t = t_0 + \tau$ is expressed as

$$d(t_0 + \tau) = d_0 \sqrt{\left| \hat{u} + \frac{\Delta \vec{r}_1(\tau) - \Delta \vec{r}_2(\tau)}{d_0} \right|^2} \simeq \begin{cases} d_0 + (\Delta \vec{r}_1(\tau) - \Delta \vec{r}_2(\tau)) \cdot \hat{u} & (\kappa \ll 1) \\ |\Delta \vec{r}_1(\tau) - \Delta \vec{r}_2(\tau)| & (\kappa \gg 1) \end{cases} \quad (42)$$

where we naturally introduce a dimensionless quantity $\kappa \equiv |\Delta \vec{r}_1(\tau) - \Delta \vec{r}_2(\tau)|/d_0$, which enables us to discriminate the short or long length and time scales for a given d_0 . Equation (42) has a clear physical interpretation; in short time scale ($\kappa \ll 1$), relevant in the change in d is the projected motion along $\vec{d}(t_0)$, while d_0 is completely irrelevant in the long time limit ($\kappa \gg 1$). For convenience, we set $\hat{u} = (1, 0, 0)$ without loss of generality. One thus finds, for a pair of independently moving probes,

$$\text{MSCD}(\tau|d_0) \simeq \begin{cases} \langle (\Delta x_1(\tau) - \Delta x_2(\tau))^2 \rangle = \frac{2}{3} \text{MSD}(\tau) & (\kappa \ll 1) \\ \langle |\Delta \vec{r}_1(\tau) - \Delta \vec{r}_2(\tau)|^2 \rangle = 2 \text{MSD}(\tau) & (\kappa \gg 1) \end{cases} \quad (43)$$

This generalizes Eq. (10); in long-time regime ($\kappa \gg 1$), $\text{MSCD}(\tau|d_0)$ is the same as $\text{MSCV}(\tau)$ and equal to twice $\text{MSD}(\tau)$. On the other hand, a reduction factor 1/3, or more generally, 1/(space dimension), appears in short-time regime ($\kappa \ll 1$), since we only count one component, i.e., along $\vec{d}(t_0)$ in the calculation. As we have seen in Sec. II B, this short-time scale behavior dominates after averaging over d_0 for a pair of independent probes in stationary state. Although the pair of intramolecular probes analyzed in Sec. III B belong to the same chain, their behaviors are essentially independent in the short-time scale $\tau \ll \tau_m$, as Eq. (20) implies. Hence, in both cases, one expects the relation (40). On the other hand, a pair of intramolecular probes is no longer independent of each other at $\tau \gtrsim \tau_m$, hence, $\text{MSCD}(\tau)$ as well as $\text{MSCV}(\tau)$ eventually approach a m -dependent constant value.

In Fig. 5, we show an example of MSCD analysis applied to the trajectory data obtained from molecular dynamic simulation of entangled polymer solutions. Here we employ a rather standard model of polymer solution with the chain length $N = 600$ and the monomer volume fraction $\phi = 0.1$ (see Appendix B for more details). As shown, MSD of tagged monomer exhibits rich anomalous behaviors, i.e., early $\tau^{1/2}$, subsequent slowing-down, a signature of the reptation dynamics ($\text{MSD} \sim \tau^{1/4}$) that is followed by later $\tau \sim t^{1/2}$ scaling [18, 21]. In addition to MSD , we have calculated MSCD using probes on different polymers (see Fig. 2 (b)) and on the same polymer (see Fig. 2 (d)). We have also calculated MSCD_c from the distance analysis between a probe and the center of mass of the system (see Fig. 2 (c)). It is remarkable that all these quantities can be mapped to MSD quite accurately according to the formulas (40) and (17).

B. Motional correlation

The above discussion clarifies that the relation (40) among MSCV , MSCD and MSD is generally expected for a pair of independent probes. In turn, this indicates that two-point MSD analysis can be combined with the standard MSD analysis to quantify the degree of correlation between motion of two probes. We illustrate the idea using the MSCV as a two-point MSD output. Assuming equal mobility for two probes, Eq (41) leads to the expression of displacement correlation between two probes in the time-scale τ in terms of $\text{MSD}(\tau)$ and $\text{MSCV}(\tau)$;

$$\langle \Delta \vec{r}_1(\tau) \cdot \Delta \vec{r}_2(\tau) \rangle = \text{MSD}(\tau) - \frac{\text{MSCV}(\tau)}{2} \quad (44)$$

We now apply the scheme to the intramolecular probe pair within a single Rouse chain. Let us define $W(m, \tau) \equiv \langle \Delta \vec{r}(n_1, \tau) \cdot \Delta \vec{r}(n_2, \tau) \rangle$ as the correlation between displacements in the time-scale τ of two tagged monomers separated $m = |n_1 - n_2|$ along the chain. Using Eqs. (24) and (29), we obtain

$$W(m, \tau) = ma^2 \left[\text{erf} \left(\sqrt{\frac{\tau_m}{4\tau}} \right) + \sqrt{\frac{4\tau}{\pi\tau_m}} \exp \left(-\frac{\tau_m}{4\tau} \right) \right] \quad (45)$$

In Fig. (6) (a), we plot $W(m, \tau)$ as a function of τ for three different inter-probe separations. The correlation between the probes' displacement is almost zero in the short time-scale in all cases, but starts to rise at the characteristic time-scale $\tau \simeq \tau_m$. Two probes thus do not feel each other in the time-scale $\tau < \tau_m$, but move together in longer time-scale, in which $W(m, \tau) \sim \text{MSD}(\tau)$. One can also look at $W(m, \tau)$ as a function of m for a given τ , or in the same way as a function of R_m that represents the characteristic spatial distance between two tagged monomers m -apart along the chain. With $W(0, \tau) = \text{MSD}(\tau)$, the normalized quantity $W(m, \tau)/\text{MSD}(\tau)$ represents the degree of motional correlation in the time-scale τ for two tagged monomers with spatial distance $R_m = am^{1/2}$ apart. In Fig. (6) (b), we plot $W(m, \tau)/\text{MSD}(\tau)$ as a function of R_m for three different time-scales. One can identify the characteristic "domain", whose size grows with time-scale as $\sim a\tau^{1/4}$.

In Ref. [16], a similar analysis based on two-point MSD measurement has been performed in an attempt to identify the domain size of chromatin. It should be of great interest to see how the correlation seen in real chromatin would be compared to the result for Rouse polymer, and how the deviation, if any, can be connected to the spatial organization of chromatin domain in nucleus.

C. Non-Gaussian parameter

Recently, there has been growing interest on the motion of probes in heterogeneous environment, where

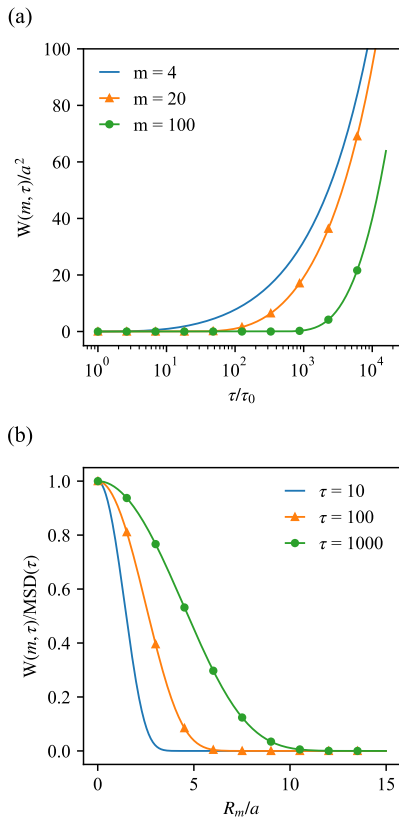


FIG. 6. Displacement correlation $W(m, \tau)$ for a pair of tagged monomers m apart along backbone in Rouse polymer. (a) $W(m, \tau)$ as a function of time-scale τ for fixed values of $m = 4, 20, 100$. (b) Normalized displacement correlation $W(m, \tau)/\text{MSD}(\tau)$ as a function of characteristic spatial distance $R_m = am^{1/2}$ between two tagged monomers for fixed values of $\tau = 10, 100, 1000$.

the statistics of probe displacement often exhibits non-Gaussian distribution [23–25]. This may be also relevant to the motion of chromatin loci in nucleus. It is therefore tempting to develop a method to quantify the non-Gaussianity within the scheme of two-point MSD. Here, we outline such a method through the distance analysis, which can be applied even when the rotational as well as the translational motion of the frame can not be neglected.

Since the short-time scale regime $\kappa \ll 1$ would eventually dominate upon averaging over d_0 , let us focus our attention on such a regime. From Eq. (42) we obtain the fourth moment of the distance change

$$\begin{aligned} \langle \Delta d(\tau)^4 \rangle &\simeq \langle (\Delta x_1(\tau) - \Delta x_2(\tau))^4 \rangle \\ &= \langle \Delta x_1(\tau)^4 \rangle + 6\langle \Delta x_1(\tau)^2 \Delta x_2(\tau)^2 \rangle + \langle \Delta x_2(\tau)^4 \rangle \end{aligned} \quad (46)$$

where we have used the independence of $\Delta x_1(\tau)$ and $\Delta x_2(\tau)$ and their third moments vanish due to symmetry. If the displacement follows the Gaussian distribution, the relation $\langle \Delta x_i(\tau)^4 \rangle = 3\langle \Delta x_i(\tau)^2 \rangle^2$ (for $i = 1, 2$) simplifies

the above equation to

$$\begin{aligned} \langle \Delta d(\tau)^4 \rangle &\xrightarrow{\text{Gaussian}} 3 [\langle \Delta x_1(\tau)^2 \rangle + \langle \Delta x_2(\tau)^2 \rangle]^2 \\ &= \frac{4}{3} [\text{MSD}(\tau)]^2 \end{aligned} \quad (47)$$

Combining with Eq. (40), this leads us to define the distance-analysis-based non-Gaussian parameter

$$\Delta_d^{\text{NG}}(\tau) \equiv \frac{\langle \Delta d(\tau)^4 \rangle}{3[\text{MSD}(\tau)]^2} - 1 \quad (48)$$

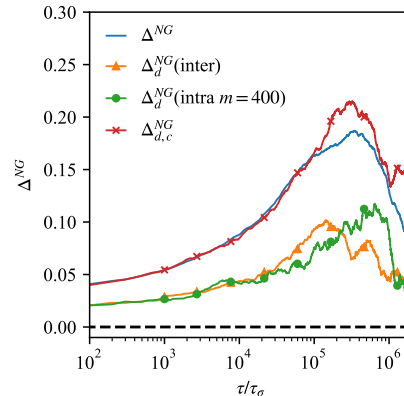


FIG. 7. Non-Gaussian parameters calculated for the molecular dynamics simulation data of entangled polymer solutions. Shown are non-Gaussian parameters calculated from Eq. (48) and Eq. (49). For the former, we employed (i) independent probe pair, (ii) intramolecular probe pair, (iii) a single probe and the center of mass to define the distance. Selection of tagged monomer(s) along each chain (with length $N = 600$) is $n = 100$, or $(n_1, n_2) = (100, 500)$ for the intramolecular pair.

We applied the analysis to the entangled linear polymer solution, in which the entanglement effect is known to cause non-Gaussian dynamics [22]. Employing the same data used in Fig. 5 (chain length $N = 600$, monomer volume fraction $\phi = 0.1$), we calculated the distance-based non-Gaussian parameter from (i) independent probe pair, (ii) intramolecular probe pair, (iii) a single probe and the center of mass. The results are shown in Fig. 6. Compared to a standard non-Gaussian parameter in single particle tracking analysis

$$\Delta^{\text{NG}}(\tau) \equiv \frac{3\langle |\Delta \vec{r}(\tau)|^4 \rangle}{5[\text{MSD}(\tau)]^2} - 1 \quad (49)$$

all the distance-based non-Gaussian parameters correctly captures the growing non-Gaussianity with the time scale and the peak position around the Rouse time $\sim \tau_0 N^2$.

In Ref. [11], authors observed the motion of chromatin loci in *C. elegans* embryo, and found a deviation from Rouse model behavior after 8 cell stage. Concomitantly, cells start to organize various characteristic intranuclear structures such as nucleolus, heterochromatin

foci, etc [10]. It would be interesting to see whether the qualitative change in loci dynamics may be associated with the possible non-Gaussian displacement statistics due to the nascent inhomogeneous nuclear environment.

V. SUMMARY

A growing need for two-point MSD has been seen in several recent experiments, in particular, those tracking chromatin loci in living cellular nucleus [8–17]. In this note, we have summarized the idea of two-point MSD, the definition of two variants MSCV and MSCD and their basic properties for a pair of independent probes as well as intramolecular probes. As is clear from their definitions, MSCD is more suitable to quantify the intrinsic mobility of the probe when the rotational motion of the container comes in. Otherwise, MSCV can be used alike.

Simple reasoning in Sect. IV A shows that the relation (40) among MSCV, MSCD and MSD generally holds for a pair of independent probes moving in free space in the stationary state. For pairs that are not independent, on the other hand, the relation (40) breaks down. In that case, one can exploit this fact by combining two-point MSD measurement with MSD, which enables us to extract and quantify the degree of motional correlation between those probe pairs (see Sec. IV B).

As necessary conditions for the relation (40), in addition to the “independence”, we put the “free space” and the “stationarity” as our analysis does not take into account the effect of the geometry of the confining space, and we also need the average over the stationary distribution of d_0 to obtain the (time averaged) MSCD. It would be interesting to see how the MSCD behaves in nonstationary, e.g., aging systems. The effect of confinement will show up when the typical displacement becomes comparable to the confinement size.

We have also proposed a way to probe non-Gaussianity in displacement statistics based on the distance analysis. We hope that the method proves to be useful in characterizing dynamics of systems embedded in moving frame as in the case of chromatin in cell nucleus.

ACKNOWLEDGEMENTS

This work was supported by JSPS KAKENHI (Grant Nos. JP23H00369, JP23H04290 and JP24K00602). We thanks A. Kimura for discussion and motivating us to summarize this note.

APPENDIX

A. Relaxation function

Here we calculate the relaxation function of the relative vector $\vec{d}(t) = \vec{r}(n_1, t) - \vec{r}(n_2, t)$ in equilibrium state. From

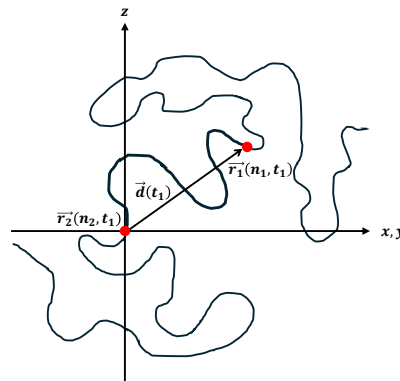


FIG. 8. Schematic representation of a polymer configuration for the “initial condition” at $t = t_1$.

the equilibrium ensemble (the canonical distribution of \vec{d} with $\langle \vec{d} \rangle = \vec{0}$), we pick up sub-ensemble of configurations that satisfy $|\vec{d}(t_1)| = d_0$, which is created by the spontaneous fluctuations. The relaxation function describes the subsequent average evolution of $\vec{d}(t)$ ($t > t_1$) in this sub-ensemble towards the equilibrium value $\vec{d} = \vec{0}$.

Without loss of generality, we assume $n_1 > n_2$ and set $\vec{r}(n_1, t_1) = (d_0/\sqrt{3})(1, 1, 1)$ and $\vec{r}(n_2, t_1) = (0, 0, 0)$. This implies the “initial condition” at time t for each Cartesian component ($\alpha = x, y, z$)

$$\langle r_\alpha(n, t_1) \rangle_{d_0} = \begin{cases} \frac{d_0}{3} & (n_1 < n) \\ \frac{n-n_2}{n_1-n_2} \frac{d_0}{3} & (n_2 < n \leq n_1) \\ 0 & (n \leq n_2) \end{cases} \quad (50)$$

where the subscript d_0 indicates the average over the sub-ensemble (Fig. 8).

From Eq. (19), the average position of n -th monomer evolves according to

$$\langle r_\alpha(n, t_1 + \tau) \rangle_{d_0} = \int dn' G(n - n', \tau) \langle r_\alpha(n', t_1) \rangle_{d_0} \quad (51)$$

Using Eq. (20) for Green function and the form (50) for the “initial condition”, we find the average position of two probe monomers as

$$\langle r_\alpha(n_1, t_1 + \tau) \rangle_{d_0} = \frac{d_0}{2\sqrt{3}} \left[\operatorname{erf} \left(\sqrt{\frac{\tau_m}{4\tau}} \right) + 1 \right] + \frac{d_0}{2\sqrt{3}\pi} \sqrt{\frac{4\tau}{\tau_m}} \left(e^{-\frac{\tau_m}{4\tau}} - 1 \right) \quad (52)$$

$$\langle r_\alpha(n_2, t_1 + \tau) \rangle_{d_0} = \frac{d_0}{2\sqrt{3}} \left[1 - \operatorname{erf} \left(\sqrt{\frac{\tau_m}{4\tau}} \right) \right] + \frac{d_0}{2\sqrt{3}\pi} \sqrt{\frac{4\tau}{\tau_m}} \left(1 - e^{-\frac{\tau_m}{4\tau}} \right) \quad (53)$$

where $\tau_m = \tau_0 m^2$ with $m = n_1 - n_2$. Equations (52) and (53) together with the definition of relaxation function in Eq. (26) leads to Eq. (28).

B. Simulation model

We employ a coarse-grained bead-spring model routinely adopted in literature, see Ref. [26] for details. Briefly, we model each polymer chain as a linear sequence of N beads of size σ . These beads are connected along the backbone by finite-extension nonlinear-elastic (FENE) bonds, and the excluded volume interactions between beads are imposed through the purely repulsive Lennard-Jones potential. We also introduce the bending potential $U_{bend}(\theta) = k_B T (l_p/a)(1 - \cos \theta)$, where θ is the angle formed between consecutive bonds, and $l_p = 5 \sigma$ is the persistence length. The polymer solution is composed of $M = 109$ polymers with length $N = 600$ in a cubic periodic box with side length $L = 87 \sigma$ such that the monomer number concentration is $0.1\sigma^{-3}$. With this concentration, polymers with $N = 600$ and $l_p = 5 \sigma$ are well entangled.

Molecular dynamics simulations are performed using the LAMMPS package [27]. The position of each bead evolves according to the under-damped Langevin equation, where the bead mass m and the friction coefficient γ are set to satisfy $m/\gamma = \gamma\sigma^2/k_B T$. The thermal noise satisfies the fluctuation dissipation theorem. To integrate the equations of motion, we employ a velocity-Verlet algorithm with time step $dt = 0.01\gamma\sigma^2/k_B T$. The length and time are measured in units of σ and $\tau_\sigma \equiv \gamma\sigma^2/k_B T$, respectively.

Let $n \in [1, N]$ denote the bead label in each polymer. In the analysis of trajectory data, we adopt one monomer $n = 100$ in each chain as tagged, and use trajectories of these tagged monomers to compute MSD, MSCD(inter) and MSCD_c in Fig. 5 and Δ^{NG} , Δ_d^{NG} (inter) and $\Delta_{d,c}^{NG}$ in Fig. 7. For the intramolecular analysis, we select two monomers $(n_1, n_2) = (100, 500)$ in each chain as tagged to compute MSCD(intra $m = 400$) in Fig. 5 and Δ_d^{NG} (intra $m = 400$) in Fig. 7.

-
- [1] H. Qian, M.P. Sheetz and E.L. Elson, *Biophys. J.* **60** 910 (1991).
- [2] R. Metzler, J.H. Jeon, A.G. Cherstvy and E. Barkai, *Phys. Chem. Chem. Phys.* **16** 24128 (2014).
- [3] H. Shen et al., *Chemical Reviews* **117**, 7331 (2017).
- [4] D.T. Clarke and M.L. Martin-Fernandez, *Methods Protoc.* **2**, 12 (2019).
- [5] W. Pönisch and V. Zaburdaev, *Eur. Phys. J. B* **91**, 27 (2018).
- [6] D.T. Gillespie and E. Seitaridou, *Simple Brownian Diffusion : An Introduction to the Standard Theoretical Models* (Oxford University Press, 2013).
- [7] M.V. Smoluchowski, *Kolloid Zeitschrift* **21**, 98 (1917).
- [8] W.F. Marshall et al., *Curr Biol.* **7**, 930 (1997).
- [9] Miné-Hattab, J., and R. Rothstein, *Nat Cell Biol.* **14**, 510 (2012).
- [10] R. Arai, T. Sugawara, Y. Sato, Y. Minakuchi, A. Toyoda, K. Nabeshima, H. Kimura, and A. Kimura, *Sci. Rep.* **7**, 3631 (2017).
- [11] A.K. Yesbolatova, R. Arai, T. Sakaue and A. Kimura, *Phys. Rev. Lett.* **128**, 178101 (2022).
- [12] N. Khanna, Y. Zhang, J.S. Lucas, O.K. Dudko and C. Murre, *Nature Communications* **10**, 2771 (2019).
- [13] M. Gabriele et al., *Science* **376**, 496 (2022).
- [14] D. B. Brückner, H. Chen, L. Barinov, B. Zoller and T. Gregor, *Science* **380**, 1357 (2023).
- [15] H. Ochiai, T. Sugawara and T. Yamamoto, *Nucleic Acids Res.* **43**, e127 (2015).
- [16] T. Nozaki et al., *Sci. Adv.* **9**, eadf1488 (2023).
- [17] K. Minami et al., *bioRxiv* 618801; doi: <https://doi.org/10.1101/2024.10.20.618801>
- [18] M. Doi and S. F. Edwards, *The Theory of Polymer Dynamics* (Clarendon Press, Oxford, 1986).
- [19] D. Panja, *J. Stat. Mech.* L02001 (2010).
- [20] T. Saito and T. Sakaue, *Phys. Rev. E* **92**, 021601 (2015).
- [21] P.-G. de Gennes, *Scaling Concepts in Polymer Physics* (Cornell University Press, Ithaca, 1979).
- [22] Z. Shen, J.-M.Y. Carrillo, B.G. Sumpter and Y. Wang, *Phys. Rev. E* **106**, 014502 (2022).
- [23] B. Wang, S.M. Anthony, S.C. Bae, and S. Granick, *Proc. Natl. Acad. Sci. U.S.A.* **106**, 15160 (2009).
- [24] M.V. Chubynsky and G.W. Slater, *Phys. Rev. Lett.* **113**, 098302 (2014).
- [25] A.V. Chechkin, F. Seno, R. Metzler and I.M. Sokolov, *Phys. Rev. X* **7**, 021002 (2017).
- [26] D. Michieletto and T. Sakaue, *ACS Macro Lett.* **10**, 129 (2021).
- [27] S. Plimpton, *J. Compu. Phys.* **117**, 1 (1995).